Real-time X-ray diffraction study through the Curie transition of the 60/40 vinylidene fluoride–trifluoroethylene copolymer as crystallized from the melt*

E. Lopez Cabarcos and A. Gonzalez Arche
Departamento de Química Física, Facultad de Farmacia, Universidad Complutense de Madrid, Madrid, Spain

F. J. Baltá Calleja
Instituto de Estructura de la Materia, CSIC, Serrano 119, 28006 Madrid, Spain

P. Bösecke, S. Röber, M. Bark and H. G. Zachmann
Institut für Technische und Makromolekulare Chemie, Universität Hamburg, Bundesstrasse 45, 2000 Hamburg 13, Germany
(Received 6 November 1989; revised 17 July 1990; accepted 7 September 1990)

Structural changes in the para-ferroelectric phase transition of the vinylidene fluoride–trifluoroethylene copolymer with 60/40 molar content have been investigated by means of real-time X-ray diffraction. A combined study of (i) long period from small-angle X-ray scattering, (ii) coherently diffracting domains derived from the integral width of the wide-angle reflections and (iii) lattice spacings offers the following picture. In the high-temperature region (65–140 C) the stacks of 250 Å thick paraelectric lamellae are found to consist of 250 Å wide coherently diffracting blocks. At the Curie transition (65–50 C) a breakdown of the large paraelectric crystals into thinner and smaller ferroelectric domains statistically mixed with the remaining paraelectric zones is observed. In the low-temperature region ($T < 50$ C), the ferroelectric phase is the predominant one (75%) though a fraction of non-polar crystals (25%) is also observed. It is further found that a part of the material in the non-polar phase can be associated with the trifluoroethylene structure, which is supported by the persistence of the corresponding reflection above the melting point of the copolymer.

(Keywords: ferroelectric copolymers; real-time X-ray diffraction; crystallization)

INTRODUCTION

The structural changes occurring in vinylidene fluoride trifluoroethylene (VDF F_3E) copolymers and their dependence on the VDF molar content have been widely investigated as a function of a variety of parameters including sample preparation, annealing effects, mechanical straining, application of electron fields, etc.[1–10]. It is now well known[11] that these copolymers exhibit a Curie transition below their melting point (T_m). At room temperature they present a ferroelectric phase that is characterized by chains in a planar all-*trans* conformation and packed in a pseudo-hexagonal lattice, similar to the β phase of PVDF[8–10]. Upon heating above the Curie temperature (T_C), the VDF F_3E copolymers undergo a structural transformation, involving a disordered sequence of conformational isomers (tg, $t\bar{g}$, tt)[1], to a centrosymmetric phase accompanied by large changes in the mechanical, electrical and thermal properties. The specific behaviour of the transition depends on the VDF content. Thus, while low VDF compositions (<40%) give a broad transition between the high-temperature phase and the non-polar phase, high VDF concentrations (>70%) show a discontinuous first-order transition in which the non-polar phase is absent[1]. A large amount of the above work, reported in characterizing the Curie transition, has been mainly done by means of wide-angle X-ray diffraction (WAXD) techniques. The information concerning the changes occurring in the superstructure as obtained from small-angle X-ray scattering (SAXS) is, however, not so abundant. Legrand has studied *in situ* the changes in the long period and lamellar orientation of drawn 70/30 samples under periodic extension[12]. Furthermore, SAXS studies on isotropic samples for various compositions (70/30, 80/20, 54/46 and 75/25) as a function of annealing temperature up to the melting point and during crystallization from the melt have also been carried out[6,13,14]. Comparison of experimental real-time scattering intensities with calculated values, derived in our laboratory[13,14] from a simple model, yielded information concerning the coexistence at the Curie transition of ferroelectric and non-ferroelectric phases within the lamellar crystals.

The main object of the present study is to supplement our previous experiments and to investigate, in real time, the changes in the small-angle X-ray scattering pattern of the 60/40 copolymer, during heating of the material to the molten state and cooling back from this state to

* Dedicated to Professor G. Martin Guzman on the occasion of his 65th birthday

0032 3861/91/173097 06

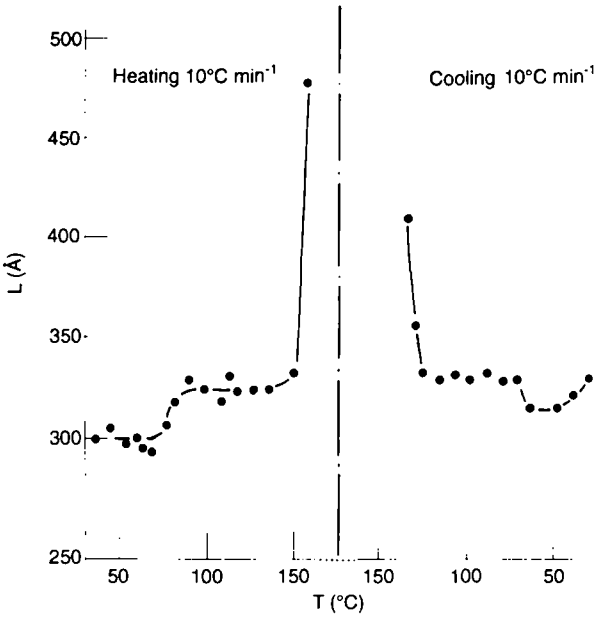

Figure 1 Long period *versus* temperature for 60/40 copolymer as derived from the SAXS maximum using Bragg's law

room temperature. The 60/40 copolymer has been selected for this investigation because the Curie transition for this composition is well defined and also because at low temperature the non-polar phase appears[1]. In addition, T_C for this copolymer lies 80°C below T_m so that structural changes can be clearly identified. Synchrotron radiation offers the possibility to record SAXS patterns instantly, which may detect temperature-induced structural changes before and during the phase transition. In this respect a combined real-time investigation of the long period from SAXS and the integral width from the wide-angle reflections was carried out on cooling from the melt, in an attempt to shed more light onto the microstructural changes occurring near the Curie transition.

EXPERIMENTAL

Commercial pellets of poly(VDF-F_3E) (60/40) from Atochem were pressure-moulded at temperatures between 160 and 180°C to 100–200 μm thick films, and the films were subsequently quenched in ice water. During X-ray diffraction experiments the resulting isotropic films were placed in a temperature chamber, melted again at 170°C for about 5 min and then cooled at a rate of 10°C min^{-1}. Thermal contact and homogeneous heating were ensured by a thin aluminium foil covering the faces of the sample. The temperature was measured by a thermocouple embedded near the sample. Wide-angle X-ray diffraction and small-angle X-ray scattering measurements were made using a double-focusing camera for synchrotron radiation on the polymer beam line at HASYLAB Hamburg[15]. The wavelength used was 0.15 nm with a bandpass of $\delta\lambda/\lambda = 5 \times 10^{-3}$. Scattering patterns were recorded every 20 s using a linear position-sensitive detector. They were corrected for fluctuations in the intensity of the primary beam and for the background. The integral breadth of the reflection, $\delta\beta$, was directly measured from the experimental profile (without correction) to make an estimate of the value for the coherently diffracting domains, $D = 1/\delta\beta$, normal to the chain direction as a function of temperature. The time required (20 s) to take a pattern as temperature varies gives an accuracy in temperature of ± 1.7°C for each diffraction pattern. An overview of the data acquisition system based on CAMAC hardware and modular software was published recently[16–18].

RESULTS

Small-angle X-ray scattering

The Curie transition was followed by means of small-angle X-ray diffraction. *Figure 1* illustrates the variation of the long period L with temperature for the heating and cooling process. The long period $L = 300$ Å remains nearly constant within experimental error in the low-temperature region, then it shows a sudden increase up to 325 Å at T_C, remaining constant again in the high-temperature region. Finally a very large L increase at about $T = 150$°C is observed. On cooling, essentially a symmetrically decreasing behaviour of L with T is observed: just below T_C one can follow the first steps of crystal nucleation showing a distinct decrease of L from 410 to 325 Å for a change from 140 to 130°C. In the high-temperature range (130–60°C) the value of $L \simeq 325$ Å remains practically constant. At $T = T_C$, L shows a small but nevertheless detectable decrease from 325 to 310 Å, confirming the stepwise behaviour of L near T_C. Finally the long period shows a gradual increase with decreasing temperature up to $L \simeq 325$ Å.

Wide-angle X-ray diffraction experiments

For additional characterization of the phase changes through the Curie transition, WAXD experiments were carried out as a function of temperature. The sample was first heated at a constant rate of 10°C min^{-1} from room temperature (30°C) up to 170°C. Then it was kept at this temperature for ~5 min and finally it was cooled down at the same heating rate (10°C min^{-1}) to room temperature. *Figure 2* illustrates a series of WAXD patterns in the range $16° < 2\theta < 21°$ following the above temperature variation. At room temperature the diffraction pattern shows a superposition of a very conspicuous broad peak associated with the ferroelectric phase centred at $2\theta = 18.97°$ ($d = 4.55$ Å) and a fainter one as a shoulder at $2\theta = 18.36°$ ($d = 4.70$ Å) corresponding to a non-polar phase (NF). The presence of this doublet was first pointed out by Yamada[19] and Lovinger[20]. It is to be noted, however, that some authors consider only a singlet when discussing copolymers with similar compositions[21]. As the temperature is increased, the intensity of the fainter (non-polar) peak increases and that of the ferroelectric maximum concurrently decreases. At the Curie temperature the ferroelectric peak disappears and only the paraelectric structure is present. On further heating the intensity of the paraelectric reflection rapidly increases until the vicinity of the melting point (T_m). Beyond T_m the appearance of a broad halo centred at 5.3 Å indicates the onset of the molten polymer phase. When the sample is cooled down the opposite process is observed. However, owing to the thermal hysteresis shown in *Figure 3*, the reappearance of the ferroelectric peak (Curie temperature) is shifted towards lower temperatures. At room temperature the diffraction pattern resembles that of the starting material. To minimize thermal history effects from the starting

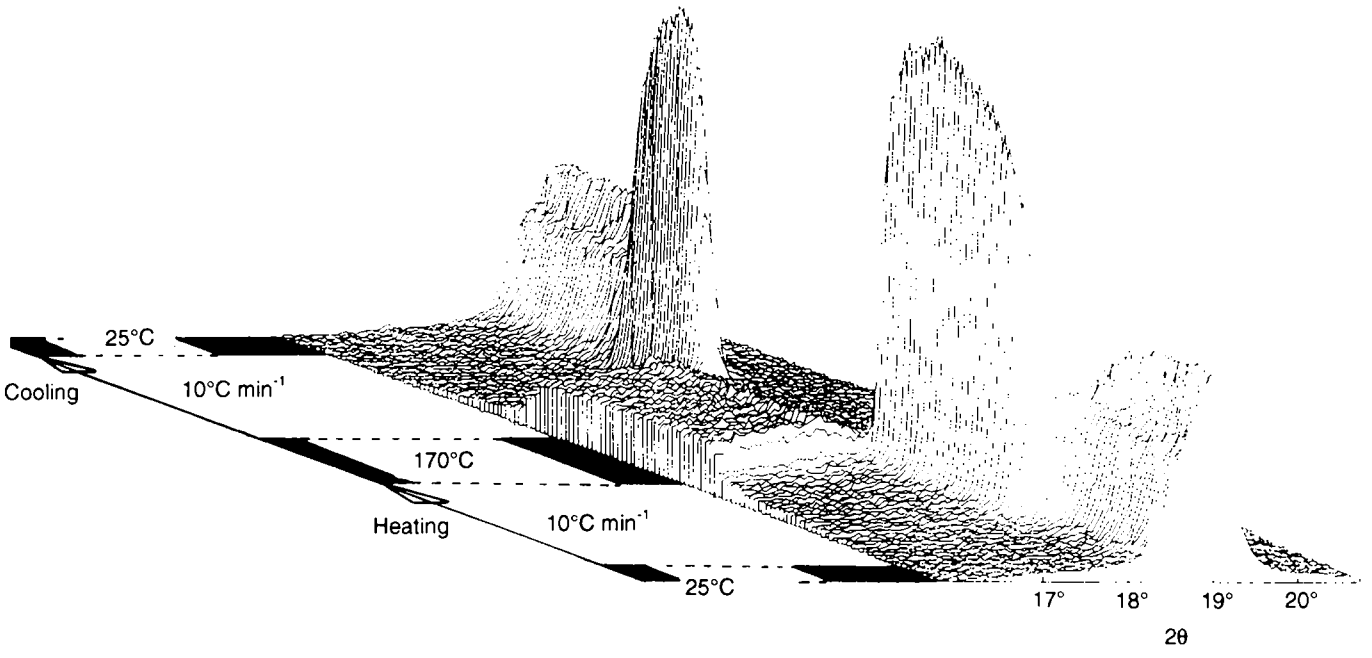

Figure 2 Three-dimensional plot of the WAXD patterns for the copolymer as a function of temperature

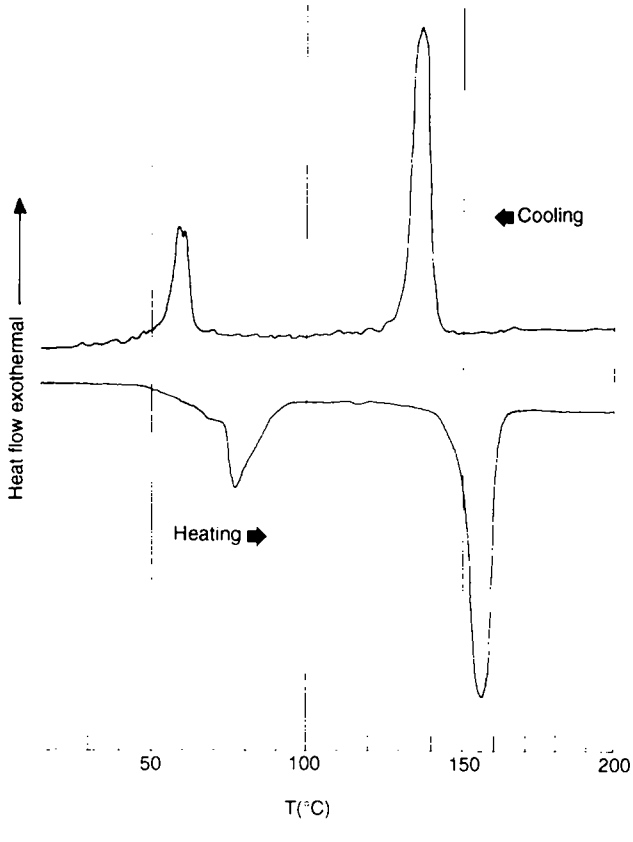

Figure 3 D.s.c. curves for the 60/40 copolymer (scanning speed 10 °C min^{-1}) showing the para–ferroelectric transition (left) and the melting and crystallization peaks (right) during the heating and cooling cycles

polymer, in the present study we have just investigated the crystallization of samples from the melt and the changes at the Curie transition occurring during the cooling process from the melt.

The study of the lattice spacings permits one to follow accurately the para–ferroelectric transition. *Figure 4a* illustrates the constancy in the spacing of the amorphous halo d_a, at about 5.3 Å, for 5 min at $T = 170$ °C (molten state) and in the temperature range 170–150 °C. Below 150 °C, crystallization takes place and the reflection corresponding to the spacing of the paraelectric phase, $d_P \simeq 5$ Å, appears. In the temperature region 150–60 °C (to be called the high-temperature range) d_P decreases linearly with T. The linear expansion coefficient α is equal to $\alpha = 0.36 \times 10^{-3}$ K^{-1}. At $T \simeq 65$ °C (Curie temperature) not only does a new spacing, d_F, corresponding to the ferroelectric phase appear but also a small fraction of the initial paraelectric crystals are gradually transformed into a new non-ferroelectric phase with a spacing that we shall denote d_{NF}. Finally, in the 50–25 °C range (low-temperature range) the spacings d_F and d_{NF} corresponding to two coexisting phases are observed; the rate for d_{NF} decrease is about 0.2×10^{-3} K^{-1} and that of d_F is about 0.4×10^{-3} K^{-1}.

The variation of the integral width of the WAXD peaks through the Curie transition is shown in *Figure 4b*. In the high-temperature range, $\delta\beta_P$ remains nearly constant. The quoted value here of $\delta\beta_P \approx 4 \times 10^{-3}$ Å^{-1} represents, in fact, the smallest possible value given by the experimental conditions. Just before T_C is reached, $\delta\beta_P$ rapidly increases, showing a maximum value ($\delta\beta = 7.5 \times 10^{-3}$ Å^{-1}) at $T = T_C$. At this point two broad diffraction peaks corresponding to the ferroelectric and non-ferroelectric phases emerge. In the low-temperature range, both $\delta\beta_{NF}$ and $\delta\beta_F$ slightly decrease on further decreasing the temperature.

Figure 4c presents the variation of crystallinity X_c and the relative fraction contribution of the different phases X_c^P, X_c^{NF} and X_c^F in the temperature range investigated through T_C. During crystallization, below $T = 150$°C, it is seen that $X_c = X_c^P$ rapidly increases with decreasing temperature and levels off at 100°C. At this temperature crystallization is completed. Most interesting is the fact that, in the 60–50 °C range (Curie transition), the volume fraction of the emerging ferroelectric (X_c^F) crystals increases linearly, while a concurrent decrease of the volume fraction of the paraelectric phase (X_c^P), which

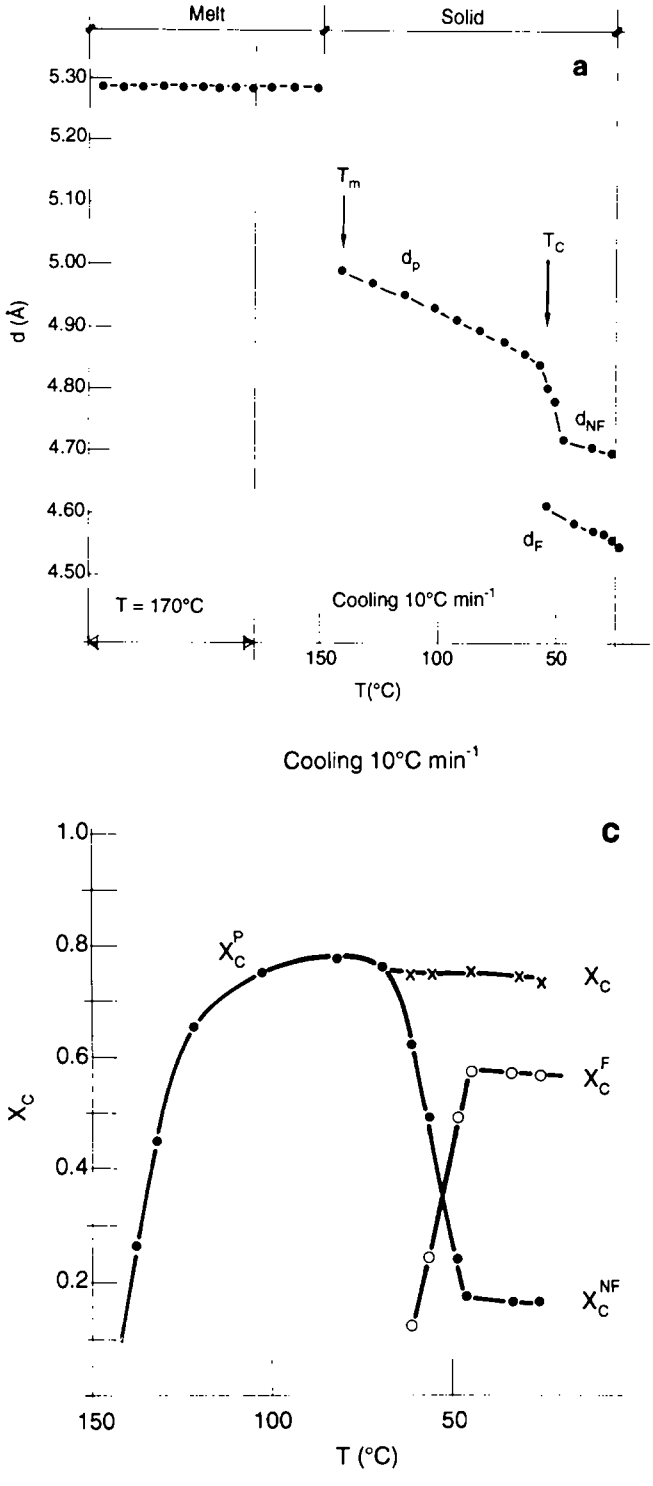

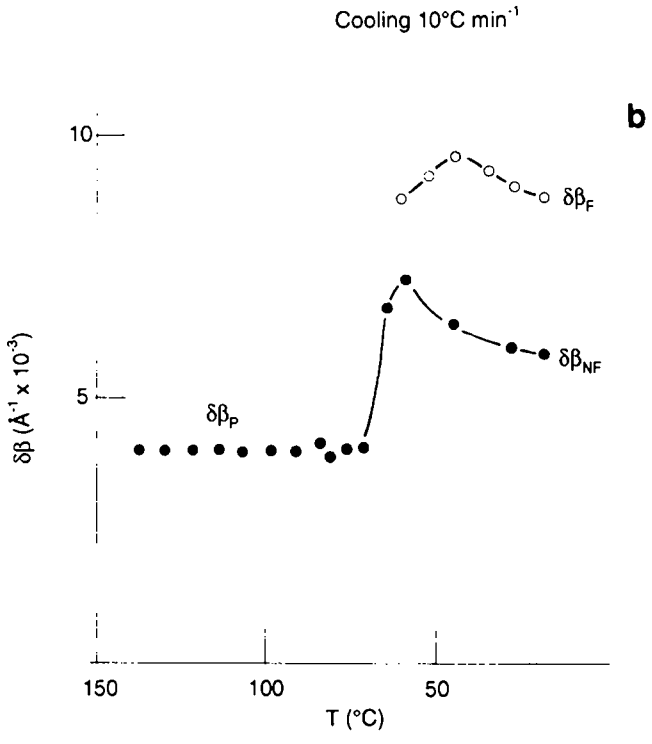

Figure 4 Variations of (a) lattice spacing d, (b) integral width $\delta\beta$ and (c) crystallinity X_c (including the crystalline ferroelectric X_c^F, non-ferroelectric X_c^{NF} and paraelectric X_c^P fractions) as functions of decreasing temperature

gradually changes into the non-ferroelectric phase in this interval, is observed. Below $T=50$°C, the ferroelectric phase predominates ($X_c^F \sim 60\%$, $X_c^{NF} \sim 18\%$), both fractions X_c^F and X_c^{NF} remaining constant.

DISCUSSION

In the high-temperature range (140 60°C) (paraelectric phase) crystallinity develops during crystallization of the material with decreasing temperature, showing a levelling-off tendency as the temperature approaches 100°C (*Figure 4c*). As can be seen in *Figure 5*, in the high-temperature range the dimensions D_P, derived from $\delta\beta$, of the emerging paraelectric coherently diffracting domains normal to the chain direction show nearly constant values ($D_P \approx 250$ Å). *Figure 5* also shows the crystal thicknesses l as derived from the X-ray long period, $l = LX_c$. It is interesting to note that when crystallization is completed, at $T \geqslant 100$°C, l is of the order of the lateral size of the crystallites D_P, in support of Wulff's rule[22] (see *Figure 6*). Simultaneously, the crystal lattice contracts with decreasing temperature in this region (*Figure 4a*), exhibiting a thermal expansion coefficient $\alpha = 0.3 \times 10^{-3}\ K^{-1}$ similar to that found in other polymers like polyethylene[23].

At $T \approx 65$°C (onset of the Curie transition) the first ferroelectric crystals appear, showing remarkably smaller lateral dimensions than the paraelectric ones (*Figures 4b* and *c*). This finding indicates that the transition above T_C involves the breakdown of paraelectric crystal blocks into smaller ferroelectric domains with dimensions D_F of about 110 Å. Evidence for the fragmentation of the paraelectric crystallites into smaller ferroelectric ones during cooling has been given previously by dark-field electron microscopy[24]. From here on ($T \simeq 65$–50°C), the increasing fraction of the new ferroelectric crystals develops at the expense of the population of paraelectric crystallites, which is linearly decreasing with T. Thus in this region (*Figure 4c*) the overall crystallinity remains nearly constant. From *Figure 3* it is evident that the para–ferroelectric phase transition is completed at T_C. The sudden decrease of the lattice spacing d_P at $T = T_C$ shown in *Figure 4a* can be associated with a transition from the paraelectric disordered phase, close to that of the melt, into a new non-ferroelectric structure (d_{NF}), which resembles that of the PF_3E homopolymer crystals. This transition parallels the simultaneous appearance of crystals having a new spacing d_F and could explain the splitting of the Curie transition endothermic peak into

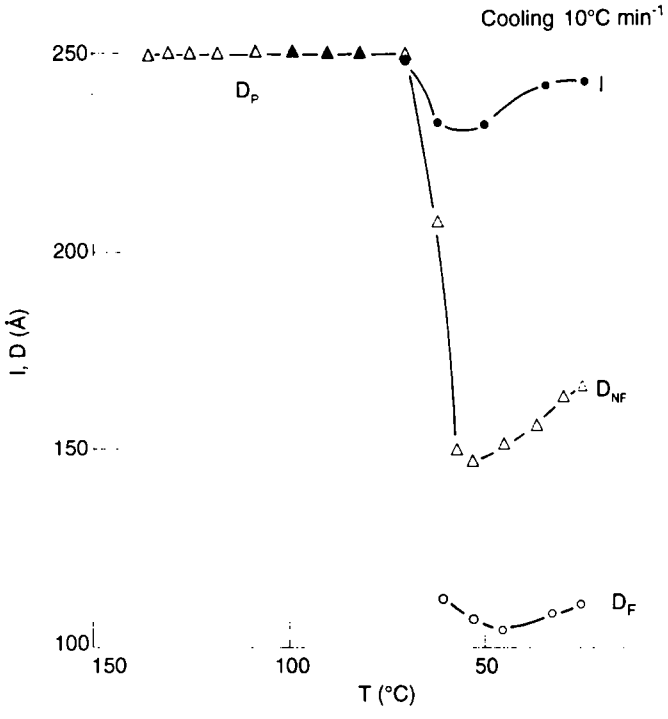

Figure 5 Dependence of the average crystal size, $l = LX_c$ and size of lateral coherently diffracting domains D_F, D_{NF} and D_P as functions of decreasing temperature

two smaller ones as seen in *Figure 3*. The average thickness of the crystalline lamellae, l, containing both ferroelectric crystalline domains and low-temperature non-ferroelectric domains, derived from $l \simeq LX_c$, slightly decreases with temperature at T_C (*Figure 5*). Simultaneously, the coherently diffracting domains for the paraelectric phase normal to the chain axis are transformed from $D_P = 250$ Å into the new non-polar crystals having dimensions of about 150 Å. The large decrease of the crystal dimension D_P seems to be directly connected with the observed sudden increase of the thermal expansion coefficient reaching a value of $\alpha = 2.5 \times 10^{-3}\ K^{-1}$ (*Figure 4a*). The increase in α is, in turn, related to the transformation of an increasing number of *gauche*-type isomers at the Curie transition into the energetically more favoured *trans* conformations. A recent study of Raman spectra for VDF F_3E copolymers with other molar contents indeed provides quantitative evidence for such *gauche–trans* conformational changes with temperature[3]. *Figure 6b* illustrates a model showing the newly formed smaller crystal blocks, of the ferroelectric phase (white regions) embedded within the lamellae of thickness l and their coexistence with the non-ferroelectric domains.

In the low-temperature range (50–25 C) the crystal dimensions l, D_{NF} and D_F show a slight parallel increase with temperature (*Figure 5*). This increase could be related to a thickening effect of the crystals towards an equilibrium state as a result of an annealing behaviour of the material when stored at these low temperatures. The population of the predominant new ferroelectric crystals and the small fraction of non-polar ones reaches an equilibrium in this temperature range (*Figure 4c*). Here the coefficient of thermal expansion of the non-ferroelectric phase is similar to that observed for the paraelectric phase in the high-temperature region ($\alpha = 0.4 \times 10^{-3}\ K^{-1}$) (*Figure 4a*).

It is known[25] that, in polymer crystals, the ratio of lateral crystal size to crystal thickness ($\mu = D/l$) exhibits values that lie between 1 and 2. However, the data of *Figure 5* show for $T < T_C$ apparently low μ values of about 0.4. This result may be related to the fact that $l = LX_c$ does not represent a coherence length but it must rather be seen as a crystal dimension that comprises a stacking of alternating ferroelectric and non-ferroelectric crystal domains. To obtain a direct estimate of the coherently diffracting crystalline dimensions along the molecular direction, the X-ray diffraction profiles in the higher wide-angle scattering region ($25 < 2\theta < 50°$) were analysed as a function of temperature. *Figure 7* shows the WAXD pattern exhibiting two maxima: a very broad maximum at a spacing $d = 2.16$ Å and a fainter peak at $d = 2.53$ Å. The latter spacing corresponds to the well known (0 0 1) reflections of the all-*trans* ferroelectric form. From the linewidth analysis, an approximate value of $D_{001} \approx 45$ Å can be derived. The ratio D_F/D_{001} now yields a value of ~ 2, which is in good agreement with Wulff's rule, indicating that the ferroelectric crystals in the low-temperature region are in an equilibrium state. The $d = 2.16$ Å spacing could be associated with a polytrifluoroethylene reflection. This reflection was first

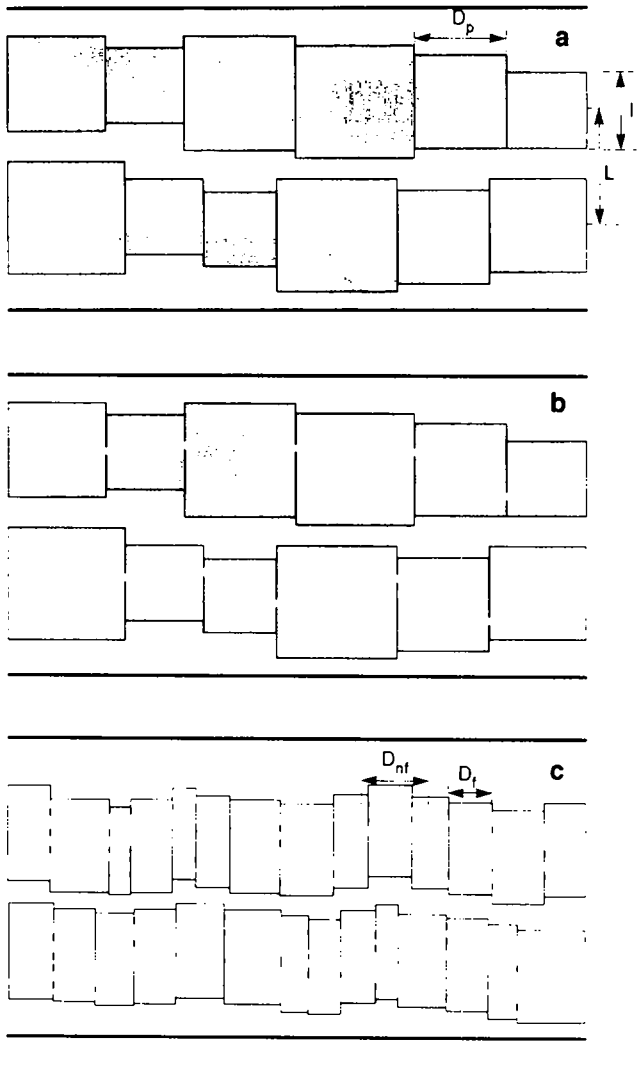

Figure 6 Schematic model of the lamellar structure of the copolymer in the (a) high-temperature range, (b) Curie transition region and (c) low-temperature range. (L and l denote respectively the long period and the average crystal thickness comprising a mixture of non-ferroelectric and ferroelectric domains

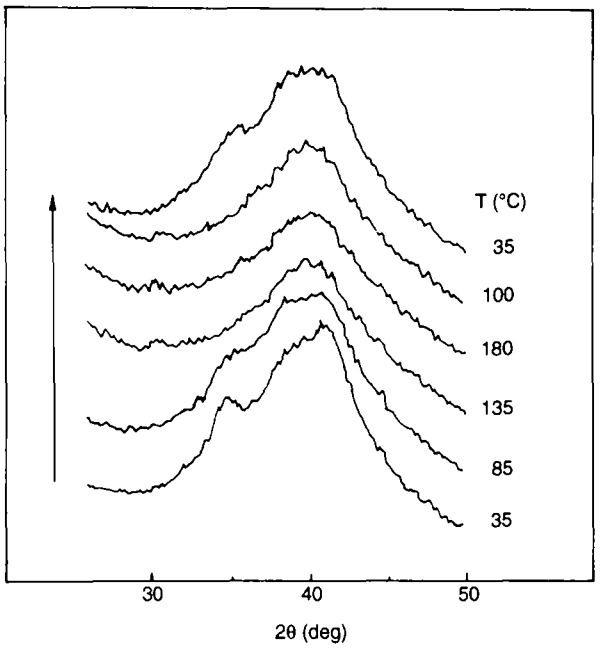

Figure 7 WAXD patterns in the angular region 30–50 (2θ) as a function of temperature

indexed by Kolda and Lando[26] as (0 0 3) and later Tashiro *et al.*[1] proposed the (2 0 1, 1 1 1) assignment. From the linewidth analysis a value of $D \simeq 12$ Å is obtained. Most revealing is the fact that with increasing temperature the (0 0 1) peak disappears while the peak at $d = 2.16$ Å prevails. These results suggest that, whereas the ferroelectric *trans* crystals are molten above $T_m \approx 155$°C, the coherently diffracting domains that correspond to the $d = 2.16$ Å spacing persist in the molten phase. One may suggest that these diffracting lengths could correspond to aggregates of trifluoroethylene short sequences having a melting temperature at about 200°C, which coexist with the non-polar phase.

CONCLUSIONS

The structural changes observed during cooling from the melt for the 60/40 copolymer can be summarized as follows:

(a) In the high-temperature region the stacks of lamellar crystals yielding a long period $L \sim 325$ Å are composed of paraelectric blocks of about 250 Å in lateral dimensions (*Figure 6a*).

(b) At the Curie temperature the large paraelectric crystals are gradually transformed into smaller ferroelectric domains ($D_F = 110$ Å, $D_{001} = 45$ Å), which become statistically mixed with the remaining non-ferroelectric zones.

(c) In the low-temperature region most of the material is transformed into the ferroelectric phase (*Figure 6c*) although a small fraction emerges as a non-polar structure. According to this model the X-ray long period below T_C comprises the alternation of crystal blocks—consisting of random coexistence of polar and non-polar domains—separated by amorphous regions.

ACKNOWLEDGEMENTS

The authors wish to express their thanks to the Internationales Büro, Kernforschungsanlage, Karlsruhe, and to Consejo Superior de Investigacions Cientificas (CSIC), Madrid, for the generous support of this Cooperation Project. Grateful acknowledgement is also due to CYCIT for the support of this investigation (grant MAT 88-0159). The measurements at HASYLAB have been partially funded by the German Federal Ministry for Research and Technology (BMFT) under the contract number 05305 HXB.

REFERENCES

1 Tashiro, K., Takano, K., Kobayashi, M., Chatani, Y. and Tadokoro, H. *Ferroelectrics* 1984, **57**, 297
2 Tashiro, K. and Kobayashi, M. *Polymer* 1986, **27**, 667
3 Tashiro, K. and Kobayashi, M. *Polymer* 1988, **29**, 426
4 Legrand, J. F., Schuele, P. J., Schmidt, V. H. and Minier, M. *Polymer* 1985, **26**, 1683
5 Lovinger, A. J., Davies, G. T., Furukawa, T. and Broadhurst, M. G. *Macromolecules* 1982, **15**, 329
6 Fernandez, M. V., Suzuki, A. and Chiba, A. *Macromolecules* 1987, **20**, 1806
7 Yagi, T. and Tatemoto, M. *Polym. J.* 1979, **11**, 429
8 Lovinger, A., Furukawa, T., Davis, G. T. and Broadhurst, M. G. *Polymer* 1983, **24**, 1225
9 Lovinger, A. *Macromolecules* 1983, **16**, 1529
10 Furukawa, T., Johnson, G. E., Bair, H. E., Tajitsu, Y., Chiba, A. and Fukada, E. *Ferroelectrics* 1981, **32**, 61
11 Koga, K. and Ohigashi, H. *J. Appl. Phys.* 1986, **59**, 2142
12 Legrand, J. F., Delzenne, P. and Lajzerowicz, J., Proc. Int. Symp. Appl. Ferroelectrics (ISAF 88) (Ed. V. Wood), Lekig University, Bethlehem, PA, 1986
13 Lopez-Cabarcos, E., Gonzalez Arche, A., Baltá Calleja, F. J. and Zachmann, H. G. *Makromol. Chem., Macromol. Symp.* 1988, **20/21**, 193
14 Lopez-Cabarcos, E., Gonzalez Arche, A., Martinez Salazar, J. and Baltá-Calleja, F. J., 'Integration of Fundamental Polymer Science and Technology', Elsevier Applied Science, London, 1988, Vol. 2, p. 193
15 Hendrix, J., Koch, M. H. J. and Bordas, J. *J. Appl. Crystallogr.* 1979, **12**, 467
16 Boulin, C., Kempf, R., Koch, M. H. J. and McLaughlin, S. M. *Nucl. Instrum. Meth. Phys. Res. (A)* 1986, **249**, 399
17 Boulin, C., Kempf, R., Gabriel, A. and Koch, M. H. J. *Nucl. Instrum. Meth. Phys. Res. (A)* 1988, **269**, 312
18 Koch, M. H. J. *Makromol. Chem., Macromol. Symp.* 1988, **15**, 79
19 Yamada, T., Ueda, T. and Kitayama, T. *J. Appl. Phys.* 1981, **52**, 948
20 Lovinger, A. J., Davis, G. T., Furukawa, T. and Broadhurst, M. G. *Macromolecules* 1982, **15**, 323
21 Tashiro, K., Takano, K., Kobayashi, M., Chatani, Y. and Tadokoro, H., *Polymer* 1984, **25**, 195
22 Hosemann, R. and Baltá Calleja, F. J. *Polymer* 1979, **20**, 1091
23 Baltá Calleja, F. J. and Vonk, C. G., 'X-Ray Scattering of Synthetic Polymers', Elsevier, Amsterdam, 1989
24 Lovinger, A. J. *Macromolecules* 1985, **18**, 910
25 Cackovic, H., Hosemann, R. and Wilke, W. *Kolloid Z. Z. Polym.* 1969, **234**, 1000
26 Kolda, R. R. and Lando, J. B. *J. Macromol. Sci., Phys. (B)* 1975, **11**(1), 21